Research Square

Preprints are preliminary reports that have not undergone peer review.
They should not be considered conclusive, used to inform clinical practice,
or referenced by the media as validated information.

Convergence, chemical transmission and co-location of sensory inputs on the C. elegans AIY interneuron: a connectome test of the semblance hypothesis

Kunjumon Vadakkan

k.vadakkan@neurosearch.ca

Neurosearch Center https://orcid.org/0000-0002-2721-6931

Research Article

Keywords: C. elegans, Caenorhabditis elegans, connectome, Learning, Associative learning, Memory, Perception, Inter-postsynaptic functional LINK

Posted Date: November 5th, 2026

DOI: https://doi.org/10.21203/rs.3.rs-11613263/v1

License: This work is licensed under a Creative Commons Attribution 4.0 International License.
Read Full License

Additional Declarations: The authors declare potential competing interests as follows: United States patent number 9477924 pertains to an electronic circuit model of the inter-postsynaptic functional LINK.

Convergence, chemical transmission and co-location of sensory inputs on the *C. elegans* AIY interneuron: a connectome test of the semblance hypothesis

Kunjumon I. Vadakkan

Neurosearch Center, Toronto, ON M6E 5A5, Canada

Correspondence: k.vadakkan@neurosearch.ca

Abstract

This study tested whether *C. elegans* has a structural signature consistent with a mechanism proposed by the semblance hypothesis: an inter-postsynaptic functional link (IPL) between closely apposed postsynaptic terminals where pathways for associatively learnable stimuli converge. In three nerve-ring reconstructions of 180–181 neurons each, the food-sensing ASE, odour-sensing AWC and temperature-sensing AFD neurons converged primarily on one interneuron, AIY, far more than expected by chance (combined $p < 10^{-9}$). As the hypothesis requires, nearly all their synapses onto AIY were chemical, more than the background electrical connectivity of AIY predicts ($p < 10^{-6}$). Because depolarization spreads along these neurites, a specific link would require direct contact, so co-location at shared reconstructed coordinates was tested. For perception, ASE terminals did not co-locate at more sites than chance, but were concentrated at a few sites on AIYR, giving about twice the expected number of ASE–ASE pairs under a synapse-level null (combined $p = 0.005$), an excess that depended on the null model. Cross-modality pairs did not exceed chance, consistent with flexible associations formed by few neurons in changing environments. Because the co-located terminals lie on a single neuron, IPL mechanisms in *C. elegans*, if present, may differ from those proposed between spines in mammals. These findings are consistent with a structural precondition predicted by the semblance hypothesis, but whether IPLs form remains to be tested.

1. Introduction

The complete synaptic wiring diagram of the 302 neurons of *C. elegans* was reconstructed by serial electron microscopy four decades ago (White et al., 1986), yet the wiring diagram alone has not explained behaviour, even in this relatively

simple organism (Bargmann and Marder, 2013). Neither anatomical connectivity nor computational descriptions of neuronal function have, by themselves, specified the physical mechanisms of circuit function (Emmons, 2016; Biswas and Fitzgerald, 2022), suggesting that an essential piece may still be missing. Drawing on constraints from many findings in mammalian systems, a theoretical approach sought a learning mechanism that can generate first-person properties during memory retrieval (Vadakkan, 2007, 2013). The postsynaptic terminal (dendritic spine) of a chemical synapse is normally kept in its resting state by continuous quantal release from its own presynaptic terminal. If two postsynaptic terminals become linked during learning by an inter-postsynaptic functional LINK (IPL), an inter-LINKed spine cannot distinguish lateral depolarization arriving through the IPL from input from its own presynaptic terminal. In this context, when one of two associatively learned stimuli reactivates the IPL, a first-person sensation of the other stimulus is generated in its absence, termed semblance (**Fig. 1A**). Perception was explained as a modified operation of IPLs in the sensory cortices (Vadakkan, 2015) (**Fig. 1B**).

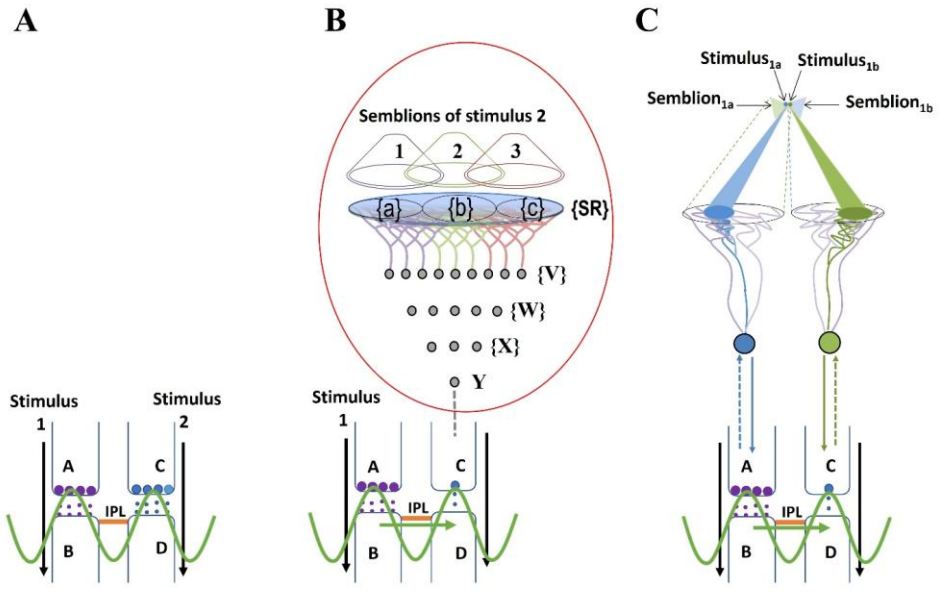


Figure 1. Inter-postsynaptic functional LINK (IPL) mechanism proposed by the semblance hypothesis. A first-person property arises when a postsynaptic terminal (spine) is depolarized through a route other than its own presynaptic terminal. **A**) During associative learning, an IPL forms between abutted spines (postsynaptic terminals) B and D onto which the sensory stimuli 1 and 2 converge. **B**) During memory retrieval, reactivation of the IPL by the cue stimulus (Stimulus

1) generates units of first-person property (semblions), whose integration forms semblance (memory). Everything within the red circle constitutes virtual first-person feature. **C**) During visual perception, stimuli from two adjacent locations on an object form an IPL and generate semblances on both inter-LINKed spines, whose integral forms percepton, unit of perception. Modified from Vadakkan, 2013, 2015.

The mean inter-spine distance on a dendritic branch exceeds the mean spine diameter (Konur et al., 2003), and sister branches often avoid overlapping (Grueber and Sagasti, 2010), raising the possibility of interaction between spines of different neurons. Abutted spines are spaced at ≤30 nm (Thorne and Nicholson, 2006; Kinney et al., 2013; Soria et al., 2020; Tønnesen et al., 2023), which theoretically allows inter-spine interaction through the extracellular space (Vadakkan, 2026). Since ≤30 nm extracellular matrix (ECM) space is near the resolution limit of real-time tracking and lies within dense neuropil (Kasthuri et al., 2015), an alternative is to look for comparable structural features in a simpler, fully reconstructed nervous system. Evolutionary continuity suggests that the capacity for internal sensation is an elaboration of an ancient circuit motif (Panksepp, 2011). If the IPL mechanism is universal, a comparable structural signature is expected even in a primitive nervous system such as that of *C. elegans*.

1.1. Criteria for IPL-equivalent features in *C. elegans*

C. elegans perceives food, odour and temperature and learns associatively: animals conditioned by pairing an odour with food later show enhanced chemotaxis toward that odour without food (Nuttley et al., 2002). Whether its simple, differently organized nervous system shows the structural logic of IPLs can therefore be asked, but its neurons differ from mammalian neurons, and these differences set four criteria used here.

1.1.1. Site. C. elegans neurons lack dendritic branches and spines and conduct signals along single, unbranched neurites, and the nerve-ring neuropil has no organized ECM (Fan et al., 2020), so interaction across ECM space cannot be assumed. Instead, sensory inputs converge onto the postsynaptic regions of a third neuron, and the membrane surface between those postsynaptic regions is taken as the IPL-equivalent site (**Fig. 2**). The nerve ring contains 181 of the 302 somatic neurons (Moyle et al., 2021), and its volumetric connectome at nanometre

resolution (Varshney et al., 2011; Jarrell et al., 2012; Cook et al., 2019; Brittin et al., 2021; Witvliet et al., 2021) allows these sites to be examined directly.

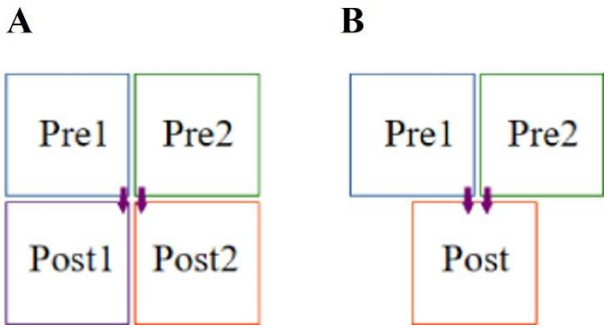


Figure 2. Suitable location for an IPL-equivalent change in *C. elegans*. Boxes are cross-sections of neurites in the nerve ring; arrows mark chemical synapses. **A**) Without an organized extracellular matrix (Fan et al., 2020), an IPL between postsynaptic sites on two different neurons (Post1 and Post2) is not expected. **B**) The membrane region between two postsynaptic sites on a third neuron (Post), where two input neurons (Pre1 and Pre2) synapse, is a suitable location for an IPL-equivalent change.

1.1.2. Convergence. If learning-related changes occur where the pathways of associated stimuli converge, ASE (food), AWC (odour) and AFD (temperature) should converge on a common postsynaptic neuron more than chance predicts. All three project to the interneuron AIY, but whether AIY is their primary site of convergence among the roughly 180 nerve-ring neurons requires a statistical test. Neurons synapse with only about one-third of the neurons they contact (N2U; computed from Brittin et al., 2021; Cook et al., 2023), so partners are selected rather than set by proximity alone. Whether convergence on AIY exceeds what physical contact allows is therefore tested first (Section 3.1).

1.1.3. Distance. C. elegans has no voltage-gated sodium channels (Bargmann, 1998), and most of its neurons signal with graded potentials rather than action potentials, with some exceptions (Mellem et al., 2008; Liu et al., 2018). Their very high input resistance (Lockery and Goodman, 2009) implies a length constant of roughly 40–140 µm. Because ASE and AWC terminals occupy only 15–34 µm of AIY (Section 3.4), depolarization at any input site is expected to spread through the whole input zone. If co-activated terminals could be linked at any separation within this zone, reactivating a link would depolarize every terminal in between,

generating non-specific semblances. Specificity requires lateral depolarization through an IPL to be confined to its partner, so the criterion is the closest separation the reconstructions resolve: zero distance, with both terminals on the same AIY profile in one section. Synapses from one presynaptic profile are always co-activated and so qualify as partners.

1.1.4. Type and stability. The hypothesis requires chemical synapses for both perception and associative learning (Vadakkan, 2013, 2015), whereas 11–12% of neuron-to-neuron connections in *C. elegans* are electrical (White et al., 1986; Varshney et al., 2011), so whether sensory inputs onto AIY are predominantly chemical is tested. Perception of a survival-critical stimulus such as food is expected to favour stable, innately formed links between postsynaptic terminals of the same modality (Vadakkan, 2015), so same-modality co-location (ASE–ASE, AWC–AWC, AFD–AFD) is examined as a candidate signature of perception. Associative links, in contrast, are expected to be short-lasting in *C. elegans* for two reasons: associations can lose relevance in a changing environment, and a small number of neurons without dendritic branches or spines may offer few combinations for IPL formation. Cross-modality co-location is therefore examined as a candidate signature of associative learning, with compound and chained structures as more lenient criteria. A co-located coordinate may represent two adjacent postsynaptic terminals or one terminal receiving two inputs; both allow depolarization through a route other than the terminal's own presynaptic terminal and are interpreted alike (**Suppl. File 2**).

2. Materials and Methods

2.1. Data sources

Real, three-dimensional (3-D) postsynaptic terminal coordinates were obtained for three independently reconstructed adult hermaphrodite specimens: N2U (Cook et al., 2019) and Witvliet Datasets 7 and 8 (Witvliet et al., 2021), giving six specimen-interneuron combinations (AIYL, AIYR × three specimens). Each synapse record includes presynaptic and postsynaptic identity, synapse type (chemical or electrical), and the 3-D position of the postsynaptic terminal. All ASE terminal coordinates are listed in **Suppl. Table S1**.

2.2. Methods

2.2.1. Tests for convergence onto AIY and synapse type

To test whether ASE, AWC and AFD converge on AIY more than chance predicts, each neuron receiving chemical synapses in each reconstruction was given a convergence score. The score was the smaller of the numbers of synapses the neuron received from ASE and from AWC, summed over the left and right members of a pair, so that only neurons receiving both inputs score highly. All neurons were ranked by score, and the score of AIY was compared with 10,000 simulations (random seed 42). In each simulation, every sensory synapse was reassigned to a neuron in contact with its presynaptic neuron, keeping each sensory neuron's synapse count; targets were weighted either by contact extent or by total synaptic input among contacted neurons. Contact was taken from measured membrane adjacency for N2U (Brittin et al., 2021) and from skeleton proximity (within 500 nm) for Witvliet 7 and 8 (**Suppl. Methods**). The same test was repeated for ASE with AFD, AWC with AFD and all three together.

Because the semblance hypothesis requires chemical synapses (Section 1.1.4), all connections from ASE, AWC and AFD onto AIY were classified as chemical or electrical. For each specimen–interneuron combination, the proportion of electrical connections among these sensory inputs was compared with that among all connections onto AIY using a one-sided Fisher's exact test, and the six *p*-values were combined (Fisher's method). Data handling is described in **Suppl. Methods**.

2.2.2. Zero-distance co-location test

For each specimen–interneuron combination, same-modality and cross-modality pairs of postsynaptic terminals at a shared coordinate were counted, treating each recorded synapse, including repeated records from one presynaptic profile, as a separate terminal. A shared coordinate means that both synapses were annotated onto the same AIY profile in one electron-microscopy section (section step 80, 50 and 30 nm in N2U, Witvliet 7 and Witvliet 8, respectively). Significance was assessed with an anatomy-preserving null: positions of all terminals on AIY, from any presynaptic partner, were held fixed and identity labels reshuffled 10,000 times (random seed 42); expected counts are reshuffle means, and *p*-values were combined via Fisher's method. The three same-modality tests (ASE–ASE, AWC–AWC, AFD–AFD) were the primary, hypothesis-derived tests; all other analyses

were secondary or exploratory. Robustness analyses (summing the two sides within each animal, one terminal per presynaptic profile, a pooled count, block-permutation and spatially restricted nulls, a coordinate-level count and leave-one-coordinate-out) and the triplet, compound, chained and minimum-structure analyses are described in **Suppl. Methods**.

2.2.3. Distance structure beyond zero distance

The zero-distance test was repeated with thresholds from 0 to 50 nm, and same-modality pairs within 100 to 1000 nm were tested against the same null, with AWC and AFD as controls for clustering common to any sensory input (**Suppl. Methods**).

2.2.4. Bilateral position of sensory inputs, path lengths and feedback connections

The position of each ASE and AWC terminal was measured as the path distance along the AIY skeleton from its cell-body end (Cook et al., 2019; Witvliet et al., 2021), and ipsilateral and contralateral positions were compared with a one-sided Mann–Whitney test, combined via Fisher's method. The AIYL–AIYR gap junction, the extent of AIY occupied by sensory input, feedback connections from AIY, AIZ and RIA, and the path lengths of ASE and AWC axons to AIY were measured on the same reconstructions (**Suppl. Methods**).

3. Results

3.1. ASE, AWC and AFD converge primarily on AIY, and nearly all their synapses onto it are chemical

Of the 180–181 neurons in each reconstruction of the nerve ring, which contains all synaptic partners of ASE, AWC and AFD, AIY received the most convergent ASE and AWC input in all three specimens. ASE and AWC made 37–40% and 23–33% of their chemical synapses, respectively, onto AIY. AIY's convergence score far exceeded that expected from the physical contacts of ASE and AWC in every specimen ($p < 0.0001$ in each; combined $p < 10^{-9}$; **Fig. 3A**; **Suppl. Table S6**), under both nulls and at every contact distance tested. AFD sent 72–93% of its chemical synapses to AIY, and AIY was also the top target for ASE with AFD, AWC with AFD and all three together ($p < 0.0001$ in each specimen; combined $p <$

10^{-9}; **Fig. 3A**). The convergence of food-, odour- and temperature-sensing input on AIY is therefore not a chance outcome of how the neurons contact each other.

Electrical connections made up 12.2% of all connections in the nervous system (Varshney et al., 2011) and 6.6% of all connections onto AIY (27 of 412), but only 0.9% of ASE, AWC and AFD connections onto AIY (3 of 323; **Fig. 3B**). Sensory inputs onto AIY were therefore electrical less often than AIY's inputs as a whole (combined $p < 10^{-6}$; five of six combinations individually significant; **Suppl. Result**s). None of the three gap junctions shared an AIY profile with a chemical synapse; each lay among chemical inputs from the same sensory neuron, 0.4–1.3 µm from the nearest one.

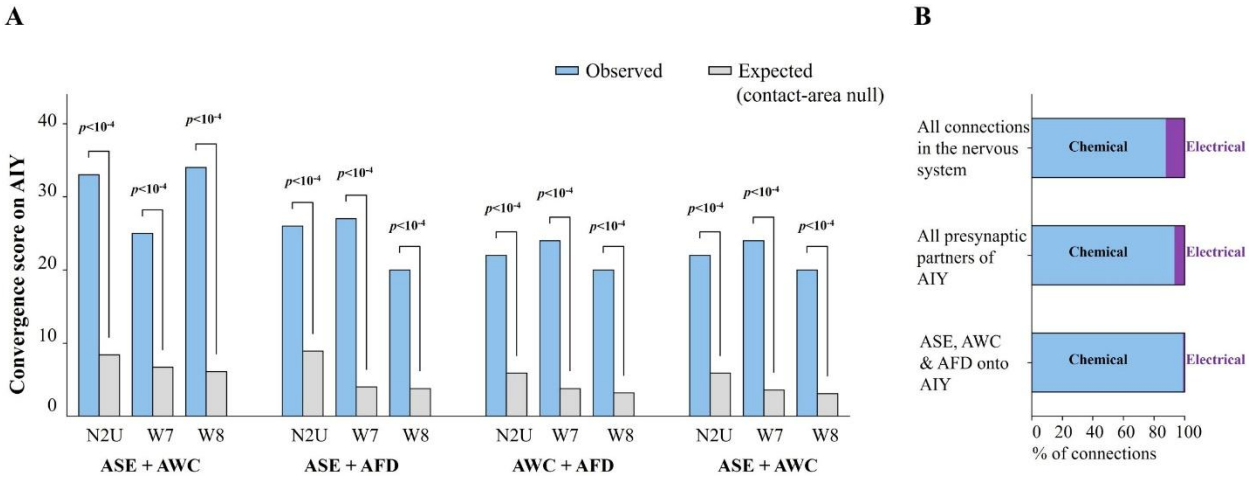


Figure 3. Convergence of sensory inputs on AIY and their synapse type. A) Convergence score on AIY (the smallest number of chemical synapses from each listed sensory pair, summed over AIYL and AIYR), observed and expected from physical contact (contact-area null; 10,000 simulations), with the *p*-value for each specimen above each pair. W7 and W8, Witvliet 7 and 8. B) Chemical and electrical connections in the whole nervous system (Varshney et al., 2011), from all presynaptic partners of AIY, and from ASE, AWC and AFD onto AIY, pooled across the six specimen–interneuron combinations.

3.2. Zero-distance co-location: dense ASE convergence at a few sites on AIYR; no cross-modality excess

3.2.1. Same-modality pairs

ASE–ASE terminal pairs shared a coordinate more often than expected under the primary per-synapse analysis (combined $p = 0.0051$; **Table 1**), driven by AIYR in N2U (18 pairs vs. 7.0 expected) and Witvliet 7 (8 vs. 2.1); no AIYL combination was significant. The result remained significant after Bonferroni correction within the three primary tests (adjusted $p = 0.015$), though not across all tests reported in this study. It also remained significant when the two sides were summed within each animal ($p = 0.003$). AWC–AWC and AFD–AFD pairs were not enriched ($p = 0.868$ and 0.479). Pooled across the six specimen–interneuron combinations, ASE–ASE pairs were 2.1 times more frequent than expected (29 vs. 13.7; $p = 0.0007$), but the 29 pairs arose from 11 coordinates, close to the 10.2 expected ($p = 0.43$; **Fig. 4**; **Suppl. Tables S1 and S7**). The excess therefore reflected dense convergence at a few sites, chiefly one N2U AIYR coordinate with five ASE terminals (10 pairs) and one Witvliet 7 AIYR coordinate with four (6 pairs); nine of the 11 sites combined ASEL and ASER terminals. Several co-located terminals were repeated synapse records from the same presynaptic profile. The excess was not significant when only one terminal per profile was counted at each coordinate (combined $p = 0.50$). When all synapses from each presynaptic profile were kept together in a block-permutation test, the pooled excess remained significant (29 vs. 15.7 expected; $p = 0.012$), but was not significant when the six combinations were combined by Fisher's method ($p = 0.14$). When spatial position, presynaptic-profile structure and synapse number were preserved together, the excess fell to about 1.25 times expected and was not significant ($p = 0.10$–0.12; **Suppl. Table S8**). Groups of three or more same-modality terminals were also not significantly enriched (ASE $p = 0.053$; **Suppl. Table S4**). These results identify a candidate spatial association whose statistical support depends on the null model; they do not establish that ASE identity, rather than the spatial arrangement and synaptic organization of the presynaptic profiles, accounts for the dense sites.

Pair type: Same-modality	ASE–ASE, $p = 0.0051$	AWC–AWC, $p = 0.868$	AFD–AFD, $p = 0.479$
Pair type: Cross-modality	ASE–AWC, $p = 0.060$	ASE–AFD, $p = 1.000$	AWC–AFD, $p = 0.986$

Table 1. Zero-distance co-location of postsynaptic terminal pairs on AIY. Fisher-combined p across the six specimen–interneuron combinations (individual values in **Suppl. Tables S2 and S3**).

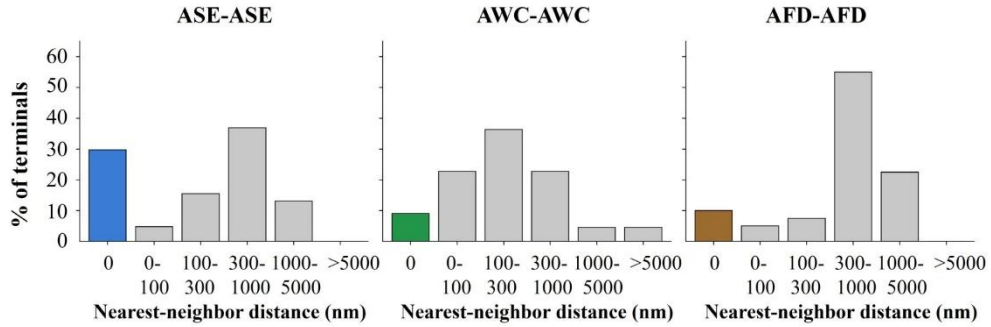


Figure 4. Nearest-neighbour postsynaptic terminal distance distributions for ASE, AWC, and AFD terminals on AIYR, pooled across all three specimens. Exact zero-distance co-location (leftmost bar in each panel) accounts for 30% of ASE terminals' nearest neighbours, compared to 9% for AWC and 10% for AFD.

3.2.2. Cross-modality pairs, compound and chained structures

No cross-modality pair type reached significance (ASE–AWC: $p = 0.060$; ASE–AFD: $p = 1.000$; AWC–AFD: $p = 0.986$; **Table 1**; **Suppl. Table S3**), and no compound or chained structure was found in any specimen, an absence consistent with chance. Where a compound structure could form, a small one of 4–6 terminals would have reached significance (**Suppl. Results**).

3.3. Distance structure beyond zero: clustering is not specific to ASE

No terminal pairs of any identity occurred between zero and each specimen's minimum non-zero separation (32–83 nm), which matches the section step (30–80 nm). The ASE result was unchanged for thresholds from 0 to 30 nm and persisted

at 100 nm, above the largest section step ($p = 0.022$), whereas AWC–AWC and AFD–AFD pairs were not enriched at either. From 350 to 1000 nm, both ASE–ASE and AWC–AWC pairs were enriched but AFD–AFD pairs were not, so clustering at these wider scales is a general feature of sensory input onto AIY (**Suppl. Table S5**).

3.4. Search for structural evidence for oscillating potentials

Brain function depends on oscillations of extracellular potentials within characteristic frequency bands (Buzsáki and Draguhn, 2004; Rusalova, 2006). Whether the circuitry around AIY has structural features that could support such activity was therefore examined. Ipsilateral ASE terminals lay closer to the AIY cell body than contralateral terminals in five of six combinations (combined $p = 0.00004$), with the two zones overlapping distally; AWC terminals showed no such order (combined $p = 0.20$). ASE and AWC terminals together occupied 15–34 µm of AIY, 54–78% of its path length from the cell body. A gap junction joined AIYL and AIYR at their distal tips in all three specimens. In all three, AIY synapsed back onto ASE directly and onto ASE and AWC through AIZ. RIA, a head interneuron that receives AIY input and controls head movement (Hendricks et al., 2012), made no synapses back onto AIY, ASE or AWC (**Fig. 5**). In the two Witvliet specimens, the ipsilateral ASE axon also reached AIY by a path 27–32 µm shorter than the contralateral axon, a lower bound because the sensory dendrites lie outside the reconstructed volumes; AWC showed the same ipsilateral advantage (29–61 µm; **Suppl. Results**).

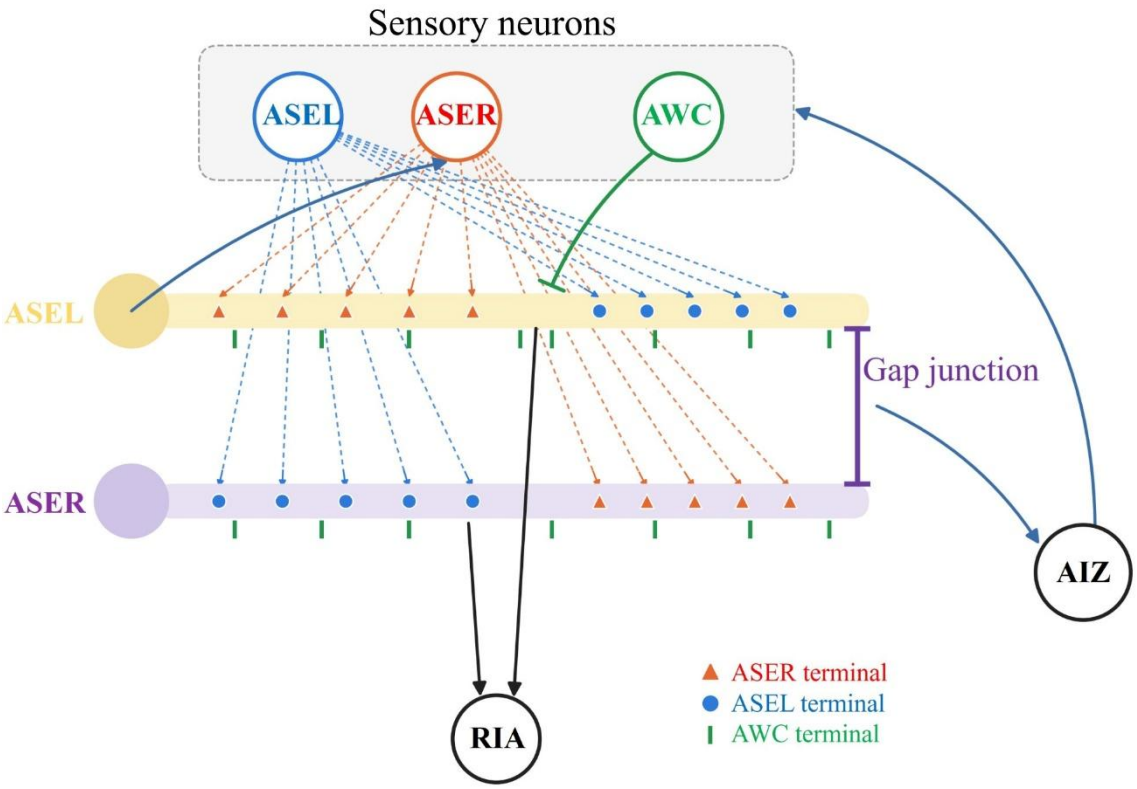


Figure 5. Arrangement of sensory inputs on AIY and the connections around it. Top: ASEL, ASER and AWC (left and right AWC combined). Middle: AIYR and AIYL drawn from the cell body (left) to the far tip (right). ASER terminals (triangles) lie closer to the cell body on AIYR and ASEL terminals (circles) on AIYL, giving a mirror-image layout; dashed arrows link each ASE neuron to its terminals (blue, ASEL; orange, ASER), and in the reconstructions the two zones partly overlap. AWC terminals (green ticks) are intermixed without this order. AWC inhibits both AIYs through glutamate-gated chloride channels (green bar), and odour relieves this inhibition (Chalasani et al., 2007). A gap junction couples the far tips of AIYL and AIYR (purple). Blue arrows show feedback chemical connections, whose sign is not known from the connectome: AIYR onto ASER (2–4 synapses per animal), AIY onto AIZ (23–37) and AIZ onto ASE and AWC (6–9). RIA receives input from both AIYs but makes no synapses back onto AIY, ASE or AWC. Only connections present in all three specimens are shown. Terminal numbers are illustrative; not to scale.

4. Discussion

The semblance hypothesis proposes that units of first-person sensation arise from a direct, membrane-level link between postsynaptic terminals of chemical synapses, during both perception and associative learning. The hypothesis specifies where, between which inputs and at what separation learning-related changes occur, predicting convergence, chemical transmission and co-location, so it can be tested anatomically. Convergence and chemical transmission were clearly met. Co-location was found only as dense convergence of food-sensing inputs at a few sites, not for cross-modality pairs. This pattern matches the distinction the hypothesis draws between perception and associative learning, but the evidence is preliminary. **Suppl. Table S9** links each prediction to its result and states the strength of the evidence.

4.1. Is the pattern consistent with the IPL mechanism specifically?

Convergence was the clearest result. Of all the neurons available, the food-, odour- and temperature-sensing neurons converged primarily on AIY, the site where the hypothesis places learning-related changes, so the choice of AIY is not an assumption but a property of the connectome. Nearly all sensory inputs onto AIY were chemical, satisfying a necessary condition of the hypothesis that is not specific to it, since chemical transmission is also expected in conventional sensory circuits. Food is arguably the most survival-critical stimulus for this organism, and the hypothesis expects a stable structure for a percept that must not fail. Consistent with this, the only co-location signature involved food-sensing ASE neurons and took the form of dense convergence at a few sites, while the number of sites did not exceed chance. No cross-modality signature was found, although cross-modality pairs were present. Since food–odour and food–temperature learning are well established in *C. elegans* (Mori and Ohshima, 1995; Nuttley et al., 2002; Torayama et al., 2007), this suggests that associative links, when formed, are not retained as stable structures in animals that have not been conditioned. The hypothesis expects associative links to remain reversible as environments change, particularly on the 2-D surface of an unbranched neurite, which offers less room than the 3-D environment of mammalian spines; the data are consistent with this expectation but cannot test it.

4.2. Clustered organization of synapses on AIY interneuron

C. elegans synapses are clustered along neurites (Ruach et al., 2023), as in clustered plasticity, in which neighbouring synapses on a dendritic branch are functionally grouped (Shepherd and Brayton, 1987; Poirazi et al., 2003; Makino and Malinow, 2011; Takahashi et al., 2012) through intracellular signals that diffuse over several micrometres (Govindarajan et al., 2006; Harvey and Svoboda, 2007). That model explains how nearby synapses change each other's strength; not how first-person sensation arises. The present data separate the two scales: clustering from 350 to 1000 nm was shared by ASE and AWC, whereas only at shared reconstructed coordinates did ASE differ from AWC and AFD. Because ASEL and ASER respond to opposite changes in salt (Suzuki et al., 2008), co-located ASEL and ASER terminals may be active together or in alternation.

4.3. Bilateral ASE–AIY circuitry: testable predictions

The mirror-image ASE layout, the tip gap junction and the feedback loops (**Fig. 5**) form a bilaterally coupled circuit. Because ASEL and ASER are driven in alternate halves of each head swing and promote opposite behaviours (Suzuki et al., 2008), and AIY controls speed and turning (Li et al., 2014), the anatomy predicts that each AIY responds earlier and more strongly to its ipsilateral ASE (**Suppl. Note**) and that AIYL and AIYR alternate, approximately in antiphase, locked to head swings. No oscillation frequency can be predicted, because the signs of the feedback synapses are unknown, apart from AWC's inhibition of AIY (Chalasani et al., 2007). Intrinsic oscillation would be shown only by activity that persists or cycles in immobilized animals exposed to steady salt. Simultaneous imaging of AIYL, AIYR and head-swing neurons during ASEL- or ASER-specific stimulation can test these predictions. Equal ipsilateral and contralateral responses or in-phase AIY activity would falsify them.

4.4. Limitations and criteria for functional confirmation

The interpretations rest on three reconstructed adult animals, and the findings are anatomical and statistical only. A shared coordinate places two terminals on the same AIY profile within one 30–80 nm section but does not show that their membranes touch, so co-location is a proxy for contact, not a measurement of it. The ASE–ASE result reflects dense convergence at a few sites and depends chiefly

on one N2U AIYR coordinate and on counting repeated synapses from one presynaptic profile separately. It was not significant under the most constrained null, although that null has limited power. The result was found on AIYR only. AIYR also had more zero-distance points of all types (30 vs. 14, 16 vs. 8, 8 vs. 1), which may reflect arrangement, annotation or the functional asymmetry of ASEL and ASER (Kuramochi and Doi, 2026). The result remains significant after correction only within the primary tests. AIYL and AIYR of one animal are not independent. The perception–learning distinction is an interpretation for testing, because no conditioned animals were reconstructed. Co-location on a neurite is an analogy for inter-spine abutment in mammals, and the true IPL distance may be smaller than the section thickness. For perception (ASE–ASE), confirming IPLs would require higher-resolution electron microscopy showing membrane apposition at co-located sites, functional imaging showing that activating one ASE input depolarizes its co-located partner more than other terminals on AIY, and evidence that disrupting this arrangement impairs food perception. For associative learning (ASE–AWC), IPL function would need to be tested in animals conditioned to pair an odour with food (Pritz et al., 2023).

5. Conclusion

In three *C. elegans* nerve-ring reconstructions, food-sensing ASE, odour-sensing AWC and temperature-sensing AFD inputs converged primarily on AIY, far more than their physical contacts predict, and nearly all their synapses onto AIY were chemical. ASE terminals were concentrated at a few shared reconstructed coordinates on AIYR, giving about twice the expected number of ASE–ASE pairs under a synapse-level null (combined $p = 0.005$). The number of co-location sites, however, did not exceed chance, and the excess depended on repeated synapses from individual presynaptic profiles. ASE inputs were also arranged in a mirror-image layout, joined by a gap junction at the AIY tips and embedded in closed feedback loops. These observations identify candidate anatomical features relevant to the semblance hypothesis but do not establish membrane apposition, IPL formation or lateral functional coupling. The absence of cross-modality enrichment does not show that associative learning leaves no persistent structure, because conditioned animals were not examined. Ultrastructural analysis, replication in additional animals, direct tests of lateral coupling and reconstruction of animals

conditioned to associate food with an odour are needed to test whether these features have the proposed significance.

Supplementary material

Suppl. File 1. Suppl. Table S1: coordinates, position along AIY and zero-distance grouping of all ASE postsynaptic terminals on AIYL and AIYR in the three specimens.

Suppl. File 2. Supplementary Rationale, Methods, Results, Note and Tables S2–S9: rationale for each test, detailed methods and results, convergence tests, co-location counts on AIY, bilateral circuitry and a summary of predictions and evidence.

Acknowledgments: The author gratefully acknowledges support from the Neurosearch Center, Toronto.

Funding: Partial funding was provided by the Neurosearch Center, Toronto.

Conflict of interest: United States patent number 9477924 pertains to an electronic circuit model of the inter-postsynaptic functional LINK.

Declaration of generative AI use in the manuscript preparation process: During the preparation of this work, the author used Claude (Anthropic) to assist with conducting statistical analysis, checking multiple sections of the manuscript and language editing.

References

Bargmann CI, Neurobiology of the *Caenorhabditis elegans* genome. Science, 282 (5396) (1998), 2028–2033, 10.1126/science.282.5396.2028

Bargmann CI, Marder E, From the connectome to brain function. Nat. Methods, 10 (6) (2013), 483–490, 10.1038/nmeth.2451

Biswas T, Fitzgerald JE, Geometric framework to predict structure from function in neural networks. Phys. Rev. Res., 4 (2) (2022), 023255, 10.1103/PhysRevResearch.4.023255

Brittin CA, Cook SJ, Hall DH, Emmons SW, Cohen N, A multi-scale brain map derived from whole-brain volumetric reconstructions. Nature, 591 (7848) (2021), 105–110, 10.1038/s41586-021-03284-x

Buzsáki G, Draguhn A, Neuronal oscillations in cortical networks. Science, 304 (5679) (2004), 1926–1929, 10.1126/science.1099745

Chalasani SH, Chronis N, Tsunozaki M, Gray JM, Ramot D, Goodman MB, Bargmann CI, Dissecting a circuit for olfactory behaviour in *Caenorhabditis elegans*. Nature, 450 (7166) (2007), 63–70, 10.1038/nature06292

Cook SJ, Jarrell TA, Brittin CA, Wang Y, Bloniarz AE, Yakovlev MA, Nguyen KCQ, Tang LT, Bayer EA, Duerr JS, Bülow HE, Hobert O, Hall DH, Emmons SW, Whole-animal connectomes of both *Caenorhabditis elegans* sexes. Nature, 571 (7763) (2019), 63–71, 10.1038/s41586-019-1352-7

Cook SJ, Kalinski CA, Hobert O, Neuronal contact predicts connectivity in the *Caenorhabditis elegans* brain. Curr. Biol., 33 (11) (2023), pp. 2315–2320, 10.1016/j.cub.2023.04.071

Emmons SW, Connectomics, the final frontier. Curr. Top. Dev. Biol., 116 (2016), 315–330, 10.1016/bs.ctdb.2015.11.001

Fan J, Ji T, Wang K, Huang J, Wang M, Manning L, Dong X, Shi Y, Zhang X, Shao Z, Colón-Ramos DA., A muscle-epidermis-glia signaling axis sustains synaptic specificity during allometric growth in *Caenorhabditis elegans*. eLife, 9 (2020), e55890, 10.7554/eLife.55890

Govindarajan A, Kelleher RJ, Tonegawa S, A clustered plasticity model of long-term memory engrams. Nat. Rev. Neurosci., 7 (7) (2006), pp. 575–583, 10.1038/nrn1937

Grueber WB, Sagasti A, Self-avoidance and tiling: mechanisms of dendrite and axon spacing. Cold Spring Harb. Perspect. Biol., 2 (9) (2010), p. a001750, 10.1101/cshperspect.a001750

Harvey CD, Svoboda K, Locally dynamic synaptic learning rules in pyramidal neuron dendrites. Nature, 450 (7173) (2007), 1195–1200, 10.1038/nature06416

Hendricks M, Ha H, Maffey N, Zhang Y, Compartmentalized calcium dynamics in a *C. elegans* interneuron encode head movement. Nature, 487 (7405) (2012), pp. 99–103, 10.1038/nature11081

Jarrell TA, Wang Y, Bloniarz AE, Brittin CA, Xu M, Thomson JN, Albertson DG, Hall DH, Emmons SW, The connectome of a decision-making neural network. Science, 337 (6093) (2012), 437–444, 10.1126/science.1221762

Kasthuri N, Hayworth KJ, Berger DR, Schalek RL, Conchello JA, Knowles-Barley S, Lee D, Vázquez-Reina A, Kaynig V, Jones TR, Roberts M, Morgan JL, Tapia JC,

Seung HS, Roncal WG, Vogelstein JT, Burns R, Sussman DL, Priebe CE, Pfister H, Lichtman JW, Saturated reconstruction of a volume of neocortex. Cell, 162 (3) (2015), 648–661, 10.1016/j.cell.2015.06.054

Kinney JP, Spacek J, Bartol TM, Bajaj CL, Harris KM, Sejnowski TJ, Extracellular sheets and tunnels modulate glutamate diffusion in hippocampal neuropil. J. Comp. Neurol., 521 (2) (2013), 448–464, 10.1002/cne.23181

Konur S, Rabinowitz D, Fenstermaker VL, Yuste R, Systematic regulation of spine sizes and densities in pyramidal neurons. J. Neurobiol., 56 (2) (2003), 95–112, 10.1002/neu.10229

Kuramochi M, Doi M, Complicated regulation of the activity of a single interneuron through rigid synaptic connections with asymmetric salt-sensory neurons in *Caenorhabditis elegans*. Neurosci. Lett., 877 (2026), 138582, 10.1016/j.neulet.2026.138582

Li Z, Liu J, Zheng M, Xu XZ, Encoding of both analog- and digital-like behavioral outputs by one *C. elegans* interneuron. Cell, 159 (4) (2014), 751–765, 10.1016/j.cell.2014.09.056

Liu Q, Kidd PB, Dobosiewicz M, Bargmann CI, *C. elegans* AWA olfactory neurons fire calcium-mediated all-or-none action potentials. Cell, 175 (1) (2018), 57–70.e17, 10.1016/j.cell.2018.08.018

Lockery SR, Goodman MB, The quest for action potentials in *C. elegans* neurons hits a plateau. Nat. Neurosci., 12 (4) (2009), 377–378, 10.1038/nn0409-377

Makino H, Malinow R, Compartmentalized versus global synaptic plasticity on dendrites controlled by experience. Neuron, 72 (6) (2011), 1001–1011, 10.1016/j.neuron.2011.09.036

Mellem JE, Brockie PJ, Madsen DM, Maricq AV, Action potentials contribute to neuronal signaling in *C. elegans*. Nat. Neurosci., 11 (8) (2008), 865–867, 10.1038/nn.2131

Mori I, Ohshima Y, Neural regulation of thermotaxis in *Caenorhabditis elegans*. Nature, 376 (6538) (1995), 344–348, 10.1038/376344a0

Moyle MW, Barnes KM, Kuchroo M, Gonopolskiy A, Duncan LH, Sengupta T, Shao L, Guo M, Santella A, Christensen R, Kumar A, Wu Y, Moon KR, Wolf G, Krishnaswamy S, Bao Z, Shroff H, Mohler WA, Colón-Ramos DA, Structural and

developmental principles of neuropil assembly in *C. elegans*. Nature, 591 (7848) (2021), 99–104, 10.1038/s41586-020-03169-5

Nuttley WM, Atkinson-Leadbeater KP, Van Der Kooy D, Serotonin mediates food-odor associative learning in the nematode *Caenorhabditis elegans*. Proc. Natl. Acad. Sci. USA, 99 (19) (2002), 12449–12454, 10.1073/pnas.192101699

Panksepp J, The basic emotional circuits of mammalian brains: do animals have affective lives? Neurosci. Biobehav. Rev., 35 (9) (2011), 1791–1804, 10.1016/j.neubiorev.2011.08.003

Poirazi P, Brannon T, Mel BW, Pyramidal neuron as two-layer neural network. Neuron, 37 (6) (2003), 989–999, 10.1016/s0896-6273(03)00149-1

Pritz C, Itskovits E, Bokman E, Ruach R, Gritsenko V, Nelken T, Menasherof M, Azulay A, Zaslaver A, Principles for coding associative memories in a compact neural network. eLife, 12 (2023), e74434, 10.7554/eLife.74434

Ruach R, Ratner N, Emmons SW, Zaslaver A, The synaptic organization in the *Caenorhabditis elegans* neural network suggests significant local compartmentalized computations. Proc. Natl. Acad. Sci. USA, 120 (3) (2023), e2201699120, 10.1073/pnas.2201699120

Rusalova MN, Frequency-amplitude characteristics of the EEG at different levels of consciousness. Neurosci. Behav. Physiol., 36 (4) (2006), 351–358, 10.1007/s11055-006-0024-x

Shepherd GM, Brayton RK, Logic operations are properties of computer-simulated interactions between excitable dendritic spines. Neuroscience, 21 (1) (1987), 151–165, 10.1016/0306-4522(87)90329-0

Soria FN, Paviolo C, Doudnikoff E, Arotcarena ML, Lee A, Danné N, Mandal AK, Gosset P, Dehay B, Groc L, Cognet L, Bezard E, Synucleinopathy alters nanoscale organization and diffusion in the brain extracellular space through hyaluronan remodeling. Nat. Commun., 11 (2020), 3440, 10.1038/s41467-020-17328-9

Suzuki H, Thiele TR, Faumont S, Ezcurra M, Lockery SR, Schafer WR, Functional asymmetry in *Caenorhabditis elegans* taste neurons and its computational role in chemotaxis. Nature, 454 (7200) (2008), 114–117, 10.1038/nature06927

Takahashi N, Kitamura K, Matsuo N, Mayford M, Kano M, Matsuki N, Ikegaya Y, Locally synchronized synaptic inputs. Science, 335 (6066) (2012), 353–356, 10.1126/science.1210362

Thorne RG, Nicholson C, *In vivo* diffusion analysis with quantum dots and dextrans predicts the width of brain extracellular space. Proc. Natl. Acad. Sci. USA, 103 (14) (2006), 5567–5572, 10.1073/pnas.0509425103

Tønnesen J, Hrabětová S, Soria FN, Local diffusion in the extracellular space of the brain. Neurobiol. Dis., 177 (2023), p. 105981, 10.1016/j.nbd.2022.105981

Torayama I, Ishihara T, Katsura I, *Caenorhabditis elegans* integrates the signals of butanone and food to enhance chemotaxis to butanone. J. Neurosci., 27 (4) (2007), pp. 741–750, 10.1523/JNEUROSCI.4312-06.2007

Vadakkan KI, Semblance of activity at the shared post-synapses and extracellular matrices: a structure function hypothesis of memory (2007), ISBN: 978-0-5954-7002-0

Vadakkan KI, A supplementary circuit rule-set for the neuronal wiring. Front. Hum. Neurosci., 7 (2013), p. 170, 10.3389/fnhum.2013.00170

Vadakkan KI, A framework for the first-person internal sensation of visual perception in mammals and a comparable circuitry for olfactory perception in *Drosophila*. SpringerPlus, 4 (2015), p. 833, 10.1186/s40064-015-1568-4

Vadakkan KI, Inter-postsynaptic functional links for associative memory: feasibility in a realistic neuropil model. J. Integr. Neurosci., 25 (9) (2026), p. 49226, 10.31083/JIN49226

Varshney LR, Chen BL, Paniagua E, Hall DH, Chklovskii DB, Structural properties of the *Caenorhabditis elegans* neuronal network. PLoS Comput. Biol., 7 (2) (2011), p. e1001066, 10.1371/journal.pcbi.1001066

White JG, Southgate E, Thomson JN, Brenner S, The structure of the nervous system of the nematode *Caenorhabditis elegans*. Philos. Trans. R. Soc. Lond. B Biol. Sci., 314 (1165) (1986), pp. 1–340, 10.1098/rstb.1986.0056

Witvliet D, Mulcahy B, Mitchell JK, Meirovitch Y, Berger DR, Wu Y, Liu Y, Koh WX, Parvathala R, Holmyard D, Schalek RL, Shavit N, Chisholm AD, Lichtman JW, Samuel ADT, Zhen M, Connectomes across development reveal principles of brain maturation. Nature, 596 (7871) (2021), pp. 257–261, 10.1038/s41586-021-03778-8

Supplementary Files

This is a list of supplementary files associated with this preprint. Click to download.

- SupplementaryFile1.xlsx
- SupplementaryFile2.docx